Military Technical College
Kobry El-Kobbah,
Cairo, Egypt

17th International Conference on Applied Mechanics and Mechanical Engineering

INTEGRATED VEHICLE CHASSIS CONTROL BASED ON DIRECT YAW MOMENT AND ACTIVE FRONT STEERING

A. Elhefnawy*, A. M. Sharaf*, H. M. Ragheb* and S. M. Hegazy*

ABSTRACT

This paper presents an advanced integrated control system which combines two fuzzy logic controllers for the Direct Yaw Moment (DYC) and Active Front Steering (AFS) in order to improve vehicle handling and cornering stability. Based on a well-developed and validated fourteen degrees of freedom full vehicle model with non-linear tire characteristics, a reference bicycle car model is introduced to compare and therefore control both the yaw rate and side slip angle of the vehicle body.

Three input variables are considered by the two controllers namely; the yaw rate, the sideslip angle, and the steering wheel angle. The control action of the direct yaw moment is carried out by generating a differential braking across the front wheels, while the control action of the active steering is carried out by modifying the steering wheel angle. The controller design is carried out by fuzzy logic which suits the non-linearity of the derived model. In addition, all necessary membership functions are given to define the linguistic variables of the input and output variables. Consequently, the correlation between input and output variables are defined by the rule base tables.

The numerical modelling is carried out through the MATLAB / Simulink environment which suits the control and optimization process. Different simulation results are carried out by considering standard test maneuvers with different driving speeds such as J-turn, fishhook, and lane change. The simulation results are compered during four cases namely, the conventional system without control, the DYC controller only, the AFS controller only and the integrated DYC and AFS controllers. The results show a substantial improvement of the vehicle stability in terms of vehicle lateral acceleration, side slip angle, yaw rate and roll angle for the developed integrated DYC and AFS controllers compared to that of the individual controller or the conventional system without control.

KEY WORDS

Active front steering (AFS), direct yaw control (DYC), fuzzy logic control

* Egyptian Armed Forces.

NOMENCLATURES

a,b	Locationof theoriginofvehicleframeofreference from front and rear axle [m]
$C_{f,r}$	Damping coefficient of front/rear suspension [N.s/m]
$C_{\alpha f,\alpha r}$	Cornering stiffness of front, rear tires [N/rad]
F_{Xi}, F_{Yi}, F_{Zi}	Tire forces expressed at vehicle frame of reference [N]
F_{xi}, F_{yi}, F_{zi}	Tire forces expressed at wheel coordinate systems [N]
g	Gravitational acceleration [m/s^2]
I_{xx}, I_{yy}, I_{zz}	Mass moment of inertia of the vehicle sprung mass [Kg.m^2]
I_{xy}, I_{yz}, I_{zx}	Mass product moment of inertia of the vehicle sprung mass [Kg.m^2]
I_{wi}	Mass moment of inertia of wheels [Kg.m^2]
$K_{f,r}$	Stiffness coefficient of front/rear suspension spring [N/m]
L	Wheelbase (distance between front and rear axle) [m]
M_{Bi}	Braking moment applied to each wheel [N.m]
M_{Di}	Driving moment applied at each wheel hub [N.m]
M_s	Sprung mass of the vehicle [Kg]
M_t	Total mass of the vehicle [Kg]
M_{Ui}	Resisting moment applied at each wheel hub [N.m]
M_{wi}	Unsprung mass at each wheel [Kg]
M_X, M_Y, M_Z	Net moments affecting the vehicle body [N.m]
p,q,r	Rotational velocities (roll, pitch and yaw) [rad/s]
$\dot{p},\dot{q},\dot{r}$	Rotational acceleration (roll, pitch and yaw) [rad/s^2]
r_{di}	Dynamic rolling radius of each wheel [m]
t_{rf}, t_{rr}	Wheel track at front and rear axle [m]
U,V,W	Translational velocities (forward, lateral and vertical) expressed at local frame of reference [m/s]
$\dot{U},\dot{V},\dot{W}$	Translational acceleration (forward, lateral and vertical) expressed at local frame of reference [m/s^2]
$Z_{bi}, \dot{Z}_{bi}$	Vertical velocities and acceleration at corners [m/s], [m/s^2]
$Z_{wi}, \dot{Z}_{wi}, \ddot{Z}_{wi}$	Wheel hub vertical position, velocity and acceleration [m], [m/s], [m/s^2]
ϕ,θ,ψ	Sprung mass angular displacement (roll, pitch and yaw) [rad]
$\omega_i, \dot{\omega}_i$	Wheel angular speed and acceleration [rad/s], [rad/s^2]

INTRODUCTION

Over the past three decades, numerous active control systems have been widely introduced to improve vehicle handling and directional stability during severe cornering maneuvers. The majority of these systems are based on regulating the tire forces in both longitudinal and lateral directions such as *Acceleration Slip Regulation* (ASR) [1, 2] , *Electronic Stability Program* (ESP) [3-6], and *Anti-lock Braking System* (ABS) [7-11]. It is widely recognized that, ESP-based systems have been proved very effectively in stability recovery at the price of perturbing the longitudinal vehicle dynamics, and possibly causing undesired longitudinal decelerations. Recently, *Active Front Steering* (AFS) has been introduced to provide an electronically controlled superposition of an angle to the steering wheel angle capable of generating corrective steering actions to enhance vehicle yaw stability [12-14]. Active Front Steering systems are capable of modifying the relation between the steering wheel angle and the tire road wheel angle at the front tires. Thus, AFS modifies the effective vehicle steering angle without changing the steering wheel position. It is less intrusive for the driver since it does not affect the longitudinal vehicle dynamics.

While each of the aforementioned control systems has its own methodology of optimizing vehicle's performance and stability, they are mostly devoted to improve a particular performance issue without considering the interactions and coupling with other electronic control systems. Additionally, the simple sum of these electronic control systems not only fails to fully reflect their specific performance, but also reduces the overall performance of the vehicle. Consequentially, the recent demand has been shifted towards the integration of vehicle control of the individual subsystems or '*Integrated Vehicle Chassis Control*' [15-24]. For this purpose, Direct Yaw Moment Control (DYC) has been recently developed to assist the driver to maintain the directional control of the vehicle. The system continuously monitors the driver's actions and compares it with the behavior of the vehicle in order to detect and counteract the vehicle tendency to loss control such as in severe under-steer or over-steer situations. For further improving vehicle handling and stability, an even better solution that allows the retention of the strong stabilization capabilities of DYC control and the fine regulation capabilities of active front steering is to design a system that integrates both controllers for stabilizing the vehicle with minimal disturbance to the longitudinal dynamics. For the integrated control of *Active Front Steering* and *Direct Yaw Moment*, several control methods can be found in the literature, such as Lyapunov method [21, 25], sliding modes [15, 16, 19], gain-scheduled linear parameter varying (LPV) control [26-28], optimal control [29]. Fuzzy logic control (FLC) is a knowledge-based control approach which simulates the human experience in controlling complex systems. FLC is mostly suitable for dynamic systems with high nonlinearities and uncertainty. Nowadays, a considerable number of work has been published to improve the vehicle lateral dynamics using FLC in particular through the integration of active front steering and active braking [17,18, 20] and [22-24].

Based on 14-DOF vehicle model incorporating nonlinear tire characteristics, this paper implements a Fuzzy Logic Controller for a combination of AFS and ESP to improve the vehicle lateral stability. The simulation results of the vehicle cornering response during double lane change maneuver are compared with that of highly sophisticated models developed in ADAMS software and well known commercial vehicle dynamic's software such as CarSim. Furthermore, an integrated control system of yaw rate and side slip angle is designed based on both the integrated Fuzzy Logic Control (FLC) for Active Front Steering control and Direct Yaw Moment control to improve the vehicle handling and stability.

MODEL DESCRIPTION

The presented work is based on a comprehensive 14 DOF full vehicle model which was developed and published by sharaf [30]. The model is less complex, yet adequate to represent vehicle dynamics accurately such that, it is possible to develop a specific vehicle sub-system with an emphasis on the modularity, flexibility and user-friendly interface. In addition, it suits the application of control systems and automatic optimization.

Sprung Mass Dynamics

The vehicle mathematical formulation embodies five masses; the vehicle sprung or body mass and four unsprung masses, which represent the assemblies of wheels, axles, and suspensions as shown in Fig. 1-a, b. The vehicle rigid body has six DOF, which includes three translations and three rotations. Based on Newton-Euler formulation, the equations of motion of the sprung mass can be written as follow [31]:

$$\Sigma F_x = m_t \cdot \left(\dot{U} - V \cdot r + W \cdot q\right) - m_s \cdot \left[x_G \cdot \left(q^2 + r^2\right) - y_G \cdot \left(p \cdot q - \dot{r}\right) - z_G \cdot \left(p \cdot r + \dot{q}\right)\right] \tag{1}$$

$$\Sigma F_y = m_t \cdot \left(\dot{V} - W \cdot p + U \cdot r\right) - m_s \cdot \left[y_G \cdot \left(r^2 + p^2\right) - z_G \cdot \left(q \cdot r - \dot{p}\right) - x_G \cdot \left(p \cdot q + \dot{r}\right)\right] \tag{2}$$

$$\Sigma F_z = m_s \cdot \left(\dot{W} - U \cdot q + V \cdot p\right) - m_s \cdot \left[z_G \cdot \left(p^2 + q^2\right) - x_G \cdot \left(p \cdot r - \dot{q}\right) - y_G \cdot \left(q \cdot r + \dot{p}\right)\right] \tag{3}$$

$$\begin{aligned}\Sigma M_x = {} & I_{xx} \cdot \dot{p} - \left(I_{yy} - I_{zz}\right) \cdot q \cdot r + I_{yz} \cdot \left(r^2 - q^2\right) - I_{zx} \cdot \left(p \cdot q + \dot{r}\right) + I_{xy} \cdot \left(p \cdot r - \dot{q}\right) \\ & + m_s \cdot y_G \cdot \left(\dot{W} - U \cdot q + V \cdot p\right) - m_s \cdot z_G \cdot \left(\dot{V} - W \cdot p + U \cdot r\right)\end{aligned} \tag{4}$$

$$\begin{aligned}\Sigma M_y = {} & I_{yy} \cdot \dot{q} - \left(I_{zz} - I_{xx}\right) \cdot p \cdot r + I_{xz} \cdot \left(p^2 - r^2\right) - I_{xy} \cdot \left(q \cdot r + \dot{p}\right) + I_{yz} \cdot \left(q \cdot p - \dot{r}\right) \\ & + m_s \cdot z_G \cdot \left(\dot{U} - V \cdot r + W \cdot q\right) - m_s \cdot x_G \cdot \left(\dot{W} - U \cdot q + V \cdot p\right)\end{aligned} \tag{5}$$

$$\begin{aligned}\Sigma M_z = {} & I_{zz} \cdot \dot{r} - \left(I_{xx} - I_{yy}\right) \cdot p \cdot q + I_{xy} \cdot \left(q^2 - p^2\right) - I_{yz} \cdot \left(r \cdot p + \dot{q}\right) + I_{zx} \cdot \left(r \cdot q - \dot{p}\right) \\ & + m_s \cdot x_G \cdot \left(\dot{V} - W \cdot p + U \cdot r\right) - m_s \cdot y_G \cdot \left(\dot{U} - V \cdot r + W \cdot q\right)\end{aligned} \tag{6}$$

$\left(\Sigma F_x\right)$ is the net force, acting on the vehicle body in the longitudinal direction. This results from the tire forces $\left(\Sigma F_{xi}\right)$ when applying driving or braking torques at the wheels, transformed from the wheel coordinate system to the body-fixed system. Both air resistance and grade resistance due to the uneven roads are also taken into account. $\left(\Sigma F_y\right)$ is the net lateral force, expressed as a projection of the net tire forces on the vehicle y-axis. $\left(\Sigma F_z\right)$ is the net force, affecting the vehicle body in the vertical direction. The effect of inclined road surfaces is taken into consideration. $\left(\Sigma M_x, \Sigma M_y, \Sigma M_z\right)$ are the external moments of the aforementioned forces about vehicle coordinates. According to SAE Recommended Practice J670e, six coordinates systems are considered namely, earth-fixed axis system, vehicle axis system and wheel axis system at each wheel.

Unsprung Mass Dynamics

The wheels are connected to the vehicle body via springs and dampers. It is assumed that each wheel has 2-DOF, one for the vertical displacement , and the other for wheel rotation as shown in Fig. 1-d. For vertical dynamics, suspension forces are calculated based on the spring stiffness , the shock absorber damping coefficient and the vertical displacement and velocity difference between the sprung mass body corner and the wheel center. The equation of motion for unsprung masses can be written as follow:

$$m_{w_i} \cdot \ddot{z}_{w_i} = m_{w_i} \cdot g + \underbrace{C_i \cdot \left(\dot{z}_{b_i} - \dot{z}_{w_i}\right) + K_i \cdot \left(z_{b_i} - z_{w_i}\right)}_{\text{Suspension Force } (F_{si})} + F_{z_i}(z) \tag{7}$$

Drivetrain Dynamics

Considering the wheel torque balance shown in Fig. 1-c and using Newton's second law for rotational dynamics, the differential equation for the spin degree-of-freedom can be obtained as follows:

$$I_{w_i} \cdot \dot{\omega}_i = M_{Di} - M_{Ui} - M_{Bi} - \left(F_{xi} \cdot r_{di}\right) \tag{8}$$

Tire Forces and Moments

In order to reflect the real dynamics of tire, a precise tire model should be adopted in handling stability control. The Magic Formula MF provides a precise tire dynamics in both linear and nonlinear region of tire [32], the common form of MF can be expressed as follows:

$$y = D \cdot \sin\left[C \cdot \arctan\left(B \cdot x - E\left(Bx - \arctan Bx\right)\right)\right] \tag{9}$$

$$Y(X) = y(x) + S_v \qquad and \qquad x = X + S_h \tag{10}$$

Where Y represents the longitudinal force, the lateral force, or the aligning torque, and X is the longitudinal slip ratio. The tire forces in longitudinal and lateral direction are calculated based on wheel longitudinal slip (λ) and slip angle (α), as follows:

$$\lambda = \frac{V_{rw} - V_{xw}}{V_{xw}} \qquad and \qquad \alpha = \frac{V_{yw}}{V_{xw}} \tag{11}$$

Where (V_{rw}) is the product of wheel rotation speed and the wheel effective radius is (R_e), (V_{xw}, V_{yw}) are the longitudinal and lateral speed of the wheel center. (B) is the stiffness factor, which is related with the initial slope; (C) is the shape factor deciding the integral shape of the tire–force curve; (D) is the peak value; (E) is the curvature factor, which controls the curvature at the peak and the horizontal position of the peak. (S_h, S_v) are the offsets of the tire force. The experiment tire force data could be used in the fitting method to get the coefficients (B ,C , D , E) in Equation (9).

$$\left.\begin{aligned} C &= b_0 \\ D &= b_1 \cdot F_z^{\,2} + b_2 \cdot F_z \\ B &= \frac{\left(b_3 \cdot F_z^{\,2} + b_4 \cdot F_z\right) \cdot e^{-b_5 \cdot F_z}}{C \cdot D} \\ E &= b_6 \cdot F_z^{\,2} + b_7 \cdot F_z + b_8 \end{aligned}\right\} \tag{12}$$

$$\left.\begin{aligned} C &= a_0 \\ D &= a_1 \cdot F_z^{\,2} + a_2 \cdot F_z \\ B &= \frac{a_3 \sin\left(2\arctan\left(F_z / a_4\right)\theta\right)\left(1 - a_5 |\gamma|\right)}{CD} \\ E &= a_6 \cdot F_z^{\,2} + a_7 \cdot F_z + a_8 \end{aligned}\right\} \tag{13}$$

The coefficients a_i (i = 0, ... ,8), b_i (i = 0, ... ,8) is calibrated through tire force tests. In this paper, the parameters B ,C , D and E are shown in Table 1, which are used to obtain the tire forces under tire nominal vertical force F_z on a certain road. However when the vehicle is steered, the vertical force is transferred among four wheels, and affects the longitudinal and lateral tire forces accordingly as given in Equation (14).

Table 1. Fitting Coefficients of the Basic Value under Nominal Conditions [32].

	B	C	D	E
Basic values for F_y	9.65	1.3	3690	-1.87
Basic values for F_x	11.45	1.62	4243	0.48

$$\left.\begin{aligned} F_{z1} &= \frac{b}{2L} m_t \cdot g - \frac{h_g}{2L} m_t \cdot a_x - \frac{bh_g}{2LC} m_t \cdot a_y \\ F_{z2} &= \frac{b}{2L} m_t \cdot g - \frac{h_g}{2L} m_t \cdot a_x + \frac{bh_g}{2LC} m_t \cdot a_y \\ F_{z3} &= \frac{a}{2L} m_t \cdot g + \frac{h_g}{2L} m_t \cdot a_x + \frac{ah_g}{2LC} m_t \cdot a_y \\ F_{z4} &= \frac{a}{2L} m_t \cdot g + \frac{h_g}{2L} m_t \cdot a_x - \frac{ah_g}{2LC} m_t \cdot a_y \end{aligned}\right\} \tag{14}$$

where a_x ,a_y are the longitudinal and lateral acceleration of the vehicle body.

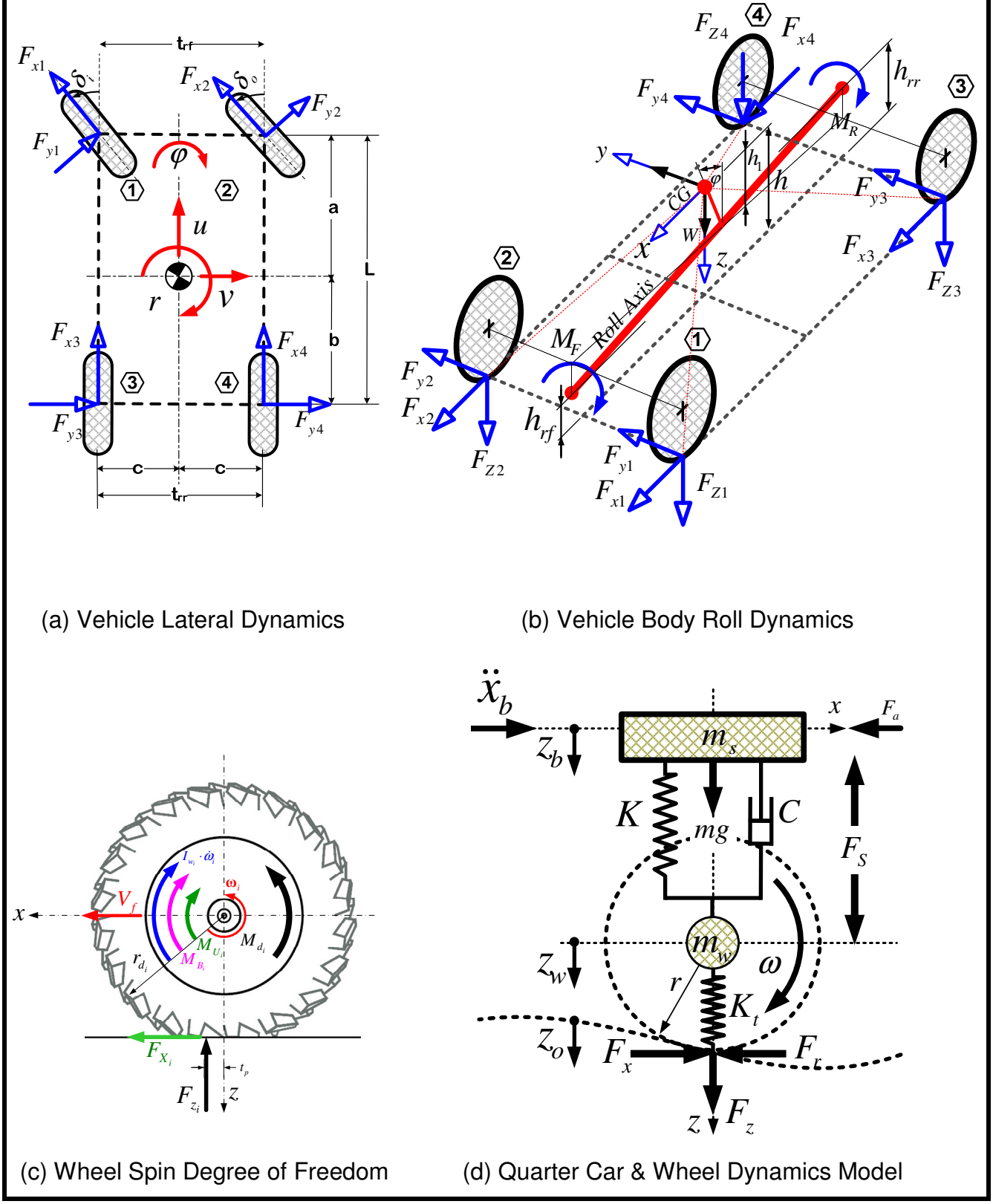

(a) Vehicle Lateral Dynamics

(b) Vehicle Body Roll Dynamics

(c) Wheel Spin Degree of Freedom

(d) Quarter Car & Wheel Dynamics Model

Fig. 1. 14-DOF Full Vehicle Mathematical Model Dynamics [30].

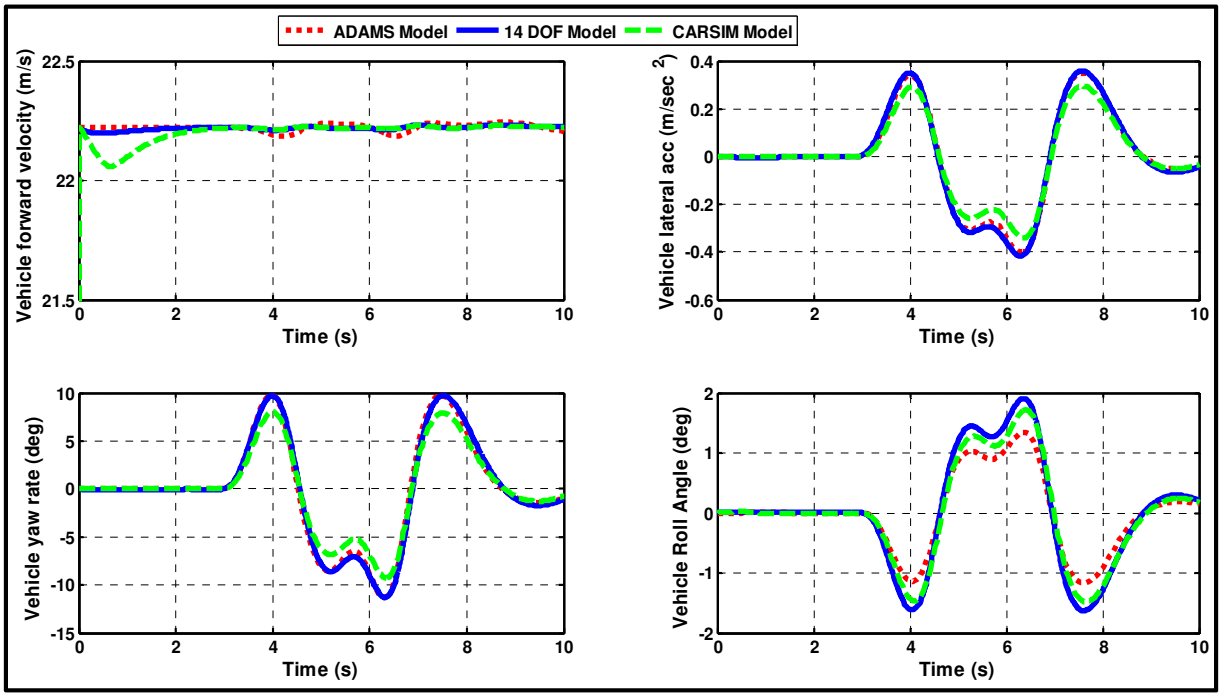

Fig. 2. The Vehicle Model Validation with ADAMS and CARSIM.

CONTROLLER DESIGN

To improve the vehicle handling and stability, the yaw rate (the yaw velocity of the chassis) and the sideslip angle (the angle between the directions of the velocity and chassis) of the vehicle are controlled to follow their desired values. A two-degrees-of-freedom (2DOF) vehicle model is adopted to calculate the desired yaw rate r_{des} as shown in Equation (15), and the desired side slip angle β_{des}, the reference of the yaw rate and the side-slip angle to the driver's steering wheel angle input and forward speed is calculated using [33]. The control system proposed in this study is shown in **Fig. 3** The reference of the yaw rate and the side-slip angle to the driver's steering wheel angle input δ and forward speed U is calculated [33].

$$r_{des} = \frac{U \cdot \delta}{\left(L + \frac{M_t \cdot U^2 \cdot \left(b \cdot c_{\alpha r} - a \cdot c_{\alpha f} \right)}{2 \cdot c_{\alpha f} \cdot c_{\alpha r} \cdot L} \right)} \tag{15}$$

The desired sideslip angle of vehicle is assumed to be zero. Both reference values are considered to improve the handling and stability of the vehicle. To obtain a desired vehicle response, it is necessary for the yaw rate and the sideslip angle to follow their target values. In this case, the main objective is to minimize the errors between the vehicle response and the desired value for both variables. The comparison of these values for each variable leads to the two required input variables

There are two outputs namely the direct yaw moment controller which takes two inputs the yaw rate error, and the side slip error, and the corrective steering angle which takes two inputs the yaw rate error, and the steering wheel angle follow:

$$\left.\begin{array}{ll} \textit{The Yaw Rate Error}: & e(r) = r - r_{des} \\ \textit{The Side Slip Angle Error}: & e(\beta) = \beta - \beta_{des} \\ \textit{The Direct Yaw Moment}: & M_{yaw} \\ \textit{The Corrective Steering Angle}: & \delta_{corr} \end{array}\right\} \quad (16)$$

Fuzzy control is a non-linear control method and can be used to deal with complicated non-linear dynamic control problems. The main advantage of fuzzy models in comparison with conventional mathematical models is the possibility of elaborating them on the basis of far lesser amounts of information about a system. Another advantage is that the use of fuzzy logic enables the heuristic rule based techniques commonly applied to be extended for use in the continuously variable situation, without significantly increasing the size of the rule base with success in many fields such as decision support, system identification, control, etc. In the last context, the number of applications of fuzzy logic to vehicle control has increased significantly over the past years with good results.

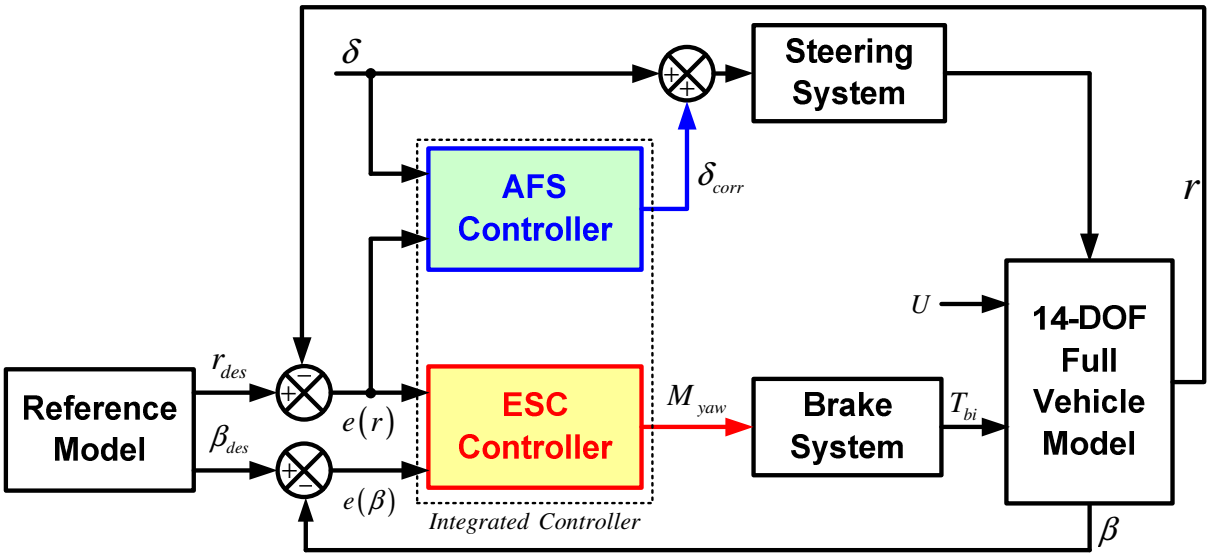

Fig. 3. Block Diagram of the Integrated Controller.

ESP Controller

ESP fuzzy controller calculates the counter direct yaw moment based on the side slip angle error and the yaw rate error. As illustrated in Fig. 4, five membership functions are selected to represent the side slip angle error, and the yaw rate error which are two trapezoidal and three triangle membership functions. On the other hand eleven membership functions are selected to represent the counter yaw moment as output of the controller which is two trapezoidal and nine triangle membership functions. The five variables for the side slip angle error and yaw rate error are namely negative big (NB), negative small (NS), zero (ZO), positive small (PS), positive big (PB). The eleven variables for the counter yaw moment are (N5, N4, N3, N2, N1, ZO, P1, P2, P3, P4, and P5). The universe of discourse for the inputs was set based on their operating range namely the side slip angle error from -6 to 6 degree, and the yaw rate error from -0.5 to 0.5 rad/sec. The direct yaw moment from fuzzy control is obtained with a scaling

factor. The rule base of the ESP Fuzzy controller is given in Table 2. The direct yaw moment DYC is generated physically from the difference in the braking between the left and right front wheels such that if the yaw moment is negative the braking torque is applied to the front left wheel and if it is positive the braking torque is applied to the front right wheel.

AFS Controller

AFS fuzzy controller calculates the corrective steering angle based on the steering wheel angle and the yaw rate error. As illustrated in Fig. 4, five membership functions are selected to represent the steering wheel angle, and the yaw rate error which are two trapezoidal and three triangle membership functions. On the other hand eleven membership functions are selected to represent the corrective steering angle as output of the controller which is two trapezoidal and nine triangle membership functions. The five variables for the steering wheel angle and the yaw rate error are namely (NB), (NS), (ZO), (PS), (PB). The eleven variables for the corrective steering angle are (N5, N4, N3, N2, N1, ZO, P1, P2, P3, P4, and P5). The universe of discourse for the inputs was set based on their operating range namely the driver steering angle from -6 to 6 rad, and the yaw rate error from -0.5 to 0.5 rad/sec. The corrective steering angle from fuzzy control is obtained with a scaling factor. The rule base of the ESP Fuzzy controller is given in table Moreover; the steering control output is added to the driver's steering. The rule base of the AFS Fuzzy controller is the same as ESP is given in Table 2.

Table 2. Fuzzy Logic Rule Base for ESP and AFS Controller.

	NB	NS	ZO	PS	PB
NB	N1	N1	ZO	P1	P1
NS	N2	N2	ZO	P2	P2
ZO	N3	N3	ZO	P3	P3
PS	N4	N4	ZO	P4	P4
PB	N5	N5	ZO	P5	P5

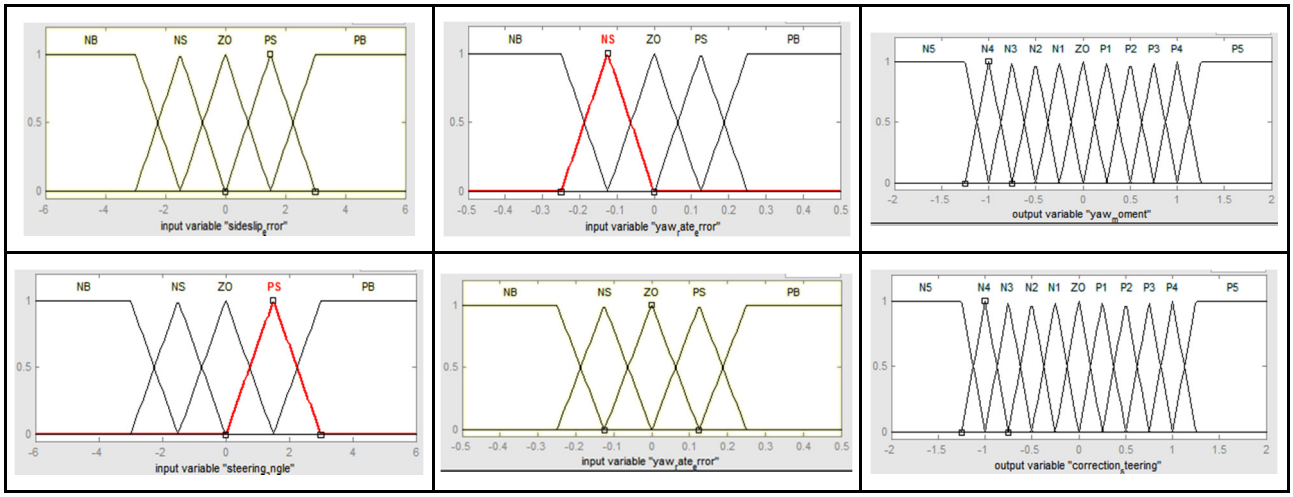

Fig. 4. Memberships Function of the Yaw Moment Controller.

MODEL SIMULATION

A numerical simulation study is conducted to show the effectiveness of the proposed controller. The 14-DOF full All-Wheel-Drive vehicle model is developed and simulated in MATLAB/ Simulink environment. The necessary parameters required by the vehicle model are given in Appendix A. The fuzzy logic controller is designed using the fuzzy logic toolbox in MATLAB/Simulink. To clarify the effects of the proposed controller, vehicle dynamics both with and without the controller are shown. The effectiveness of the controller is shown considering four different standard cornering test maneuvers at different vehicle forward velocity of 20 and 30 m/sec namely: single lane change maneuver, J-turn maneuver, fishhook maneuver, and double lane change maneuvers as shown in Fig. 5.

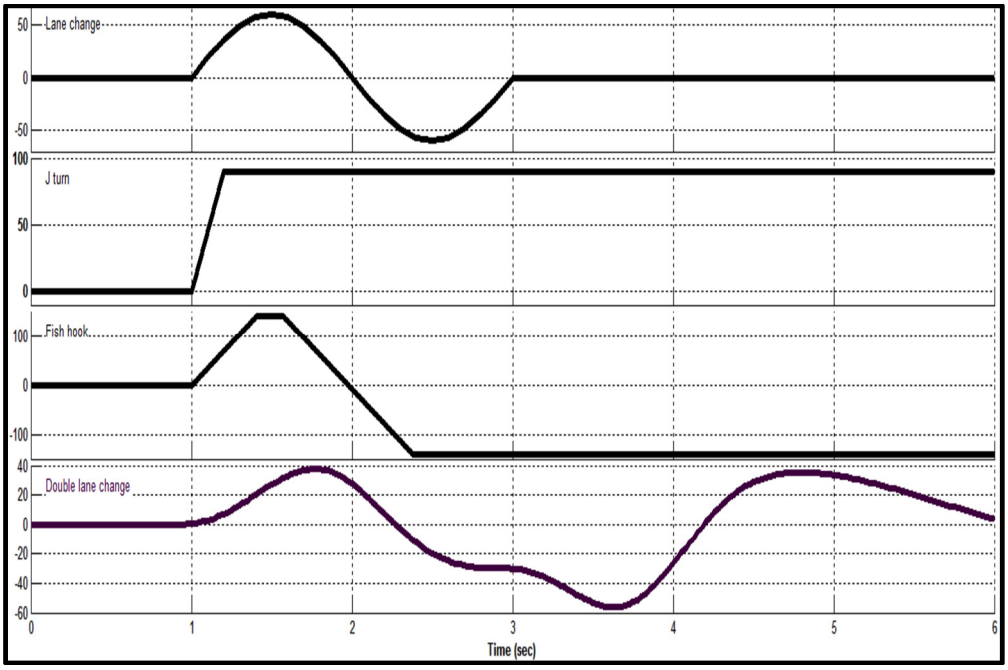

Fig. 5. Four Different Driver Steering Input in Degree.

RESULTS AND DISCUSSION

Using continuous time simulation, the simulation results are performed for a four different maneuvers inputs namely, lane change, J turn, fishhook, and double lane change at a vehicle forward velocity of 20 and 30 m/sec respectively with a nominal road friction coefficient of μ= 0.9, a value deemed to be generally representative of dry pavement.

The response of uncontrolled, AFS only, ESP only, and integrated control are shown for four stability indices performances which are lateral acceleration, roll angle, side slip angle, and yaw rate with forward vehicle velocity of 20 and 30 m/s respectively. In both cases, without a controller the vehicle stability indices performance is too large and oscillates.

Lane change maneuver is often needed to avoid obstacles in real-life situations, and it is a very useful to evaluate both the stability and handling of a vehicle as shown in Figs. 6-7. The AFS only, ESP only, and integrated controller all keep lateral acceleration, roll angle, side slip angle, and yaw rate in the desired region and have

fast rise times. However, the integrated control shows the best results. The root mean square values of the uncontrolled system, AFS only, ESP only, and integrated controller for lane change maneuver at 30 m/sec are tabulated in Table 3.

Table 3. RMS for Lane Change Steer test at 30 m/sec.

Criteria	Uncontrolled	AFS	ESP	Integrated
Lateral Acceleration	2.3441	1.8546 (**20.9%**)	1.5733 (**32.9%**)	0.9725 (**58.5%**)
Side Slip Angle	1.0857	0.7220 (**33.5%**)	0.4600 (**57.6%**)	0.25 (**77%**)
Yaw Rate	5.9135	4.4901 (**24.1%**)	3.7546 (**36.5%**)	2.3147 (**60.9%**)
Roll Angle	1.4653	1.1492 (**21.6%**)	0.9643 (**34.2%**)	0.593 (**59.6%**)

It is clear from Fig. 6 that both AFS and the ESP have almost the same effect with a little time delay in ESP controller, but from Fig. 7, ESP controller provides a great effect in reducing the amplitude of the oscillation.

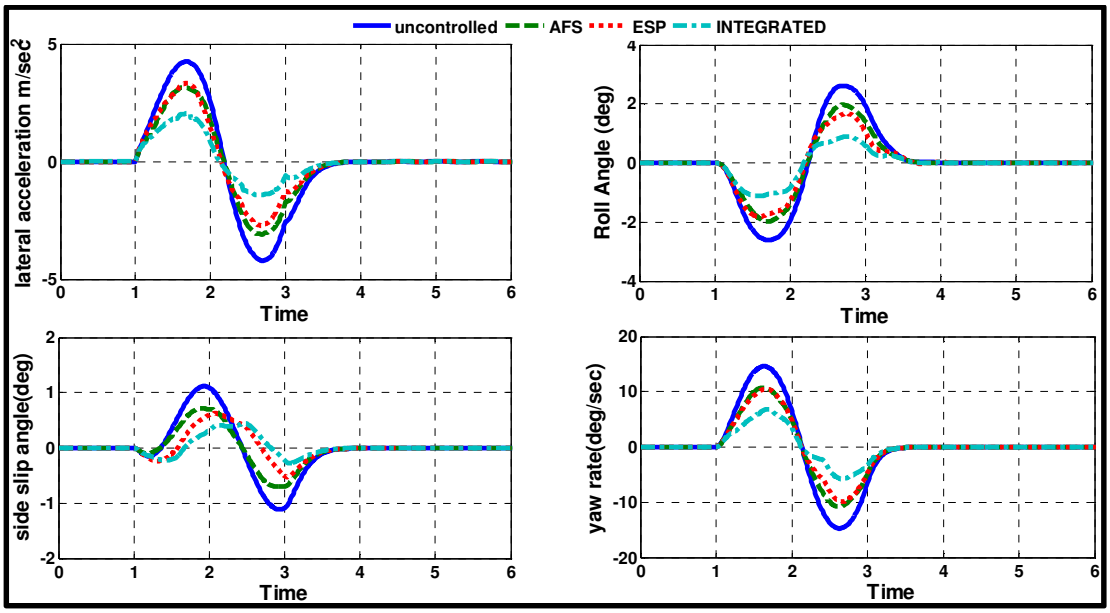

Fig. 6. Vehicle Response during Lane Change with Speed 20 m/s.

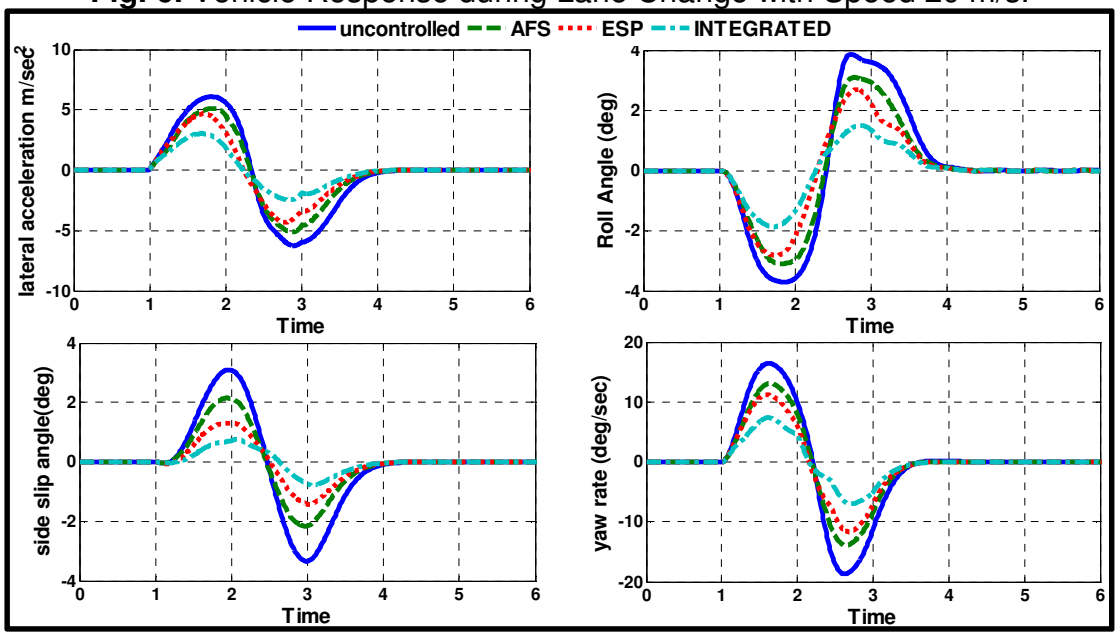

Fig. 7. Vehicle Response during Lane Change with Speed 30 m/s.

Figs. 8-9 show the vehicle response for uncontrolled system, AFS only, ESP only, and integrated controller during J-turn maneuver with maximum angle of 90 degree at speed 20 and 30 m/s respectively. The root mean square values of the uncontrolled system, AFS only, ESP only, and integrated controller for J turn maneuver at 30 m/s are tabulated in Table 4, the percentage of improvement relative to uncontrolled values is given in brackets. Based on the simulation results, stability indices performance are greatly improved with the integrated and ESP only control, and the AFS control effect diminish at high lateral acceleration as shown in Fig. 8.

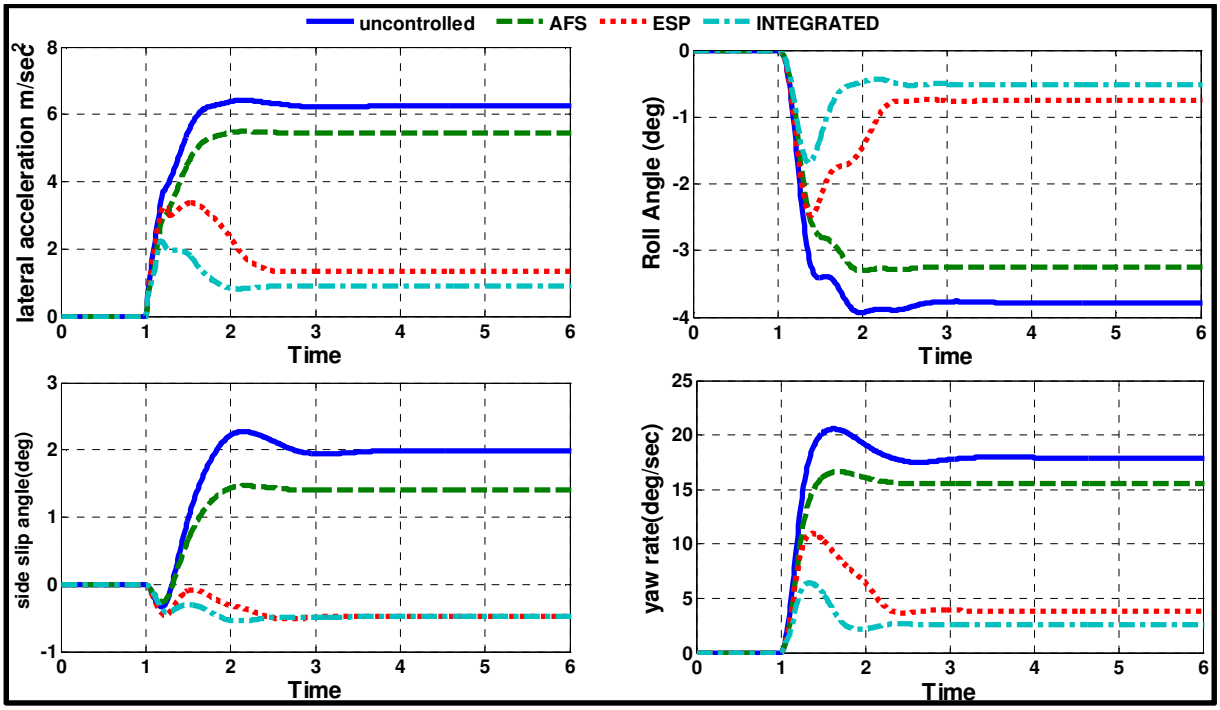

Fig. 8. Vehicle Response during J- turn with Speed 20 m/s.

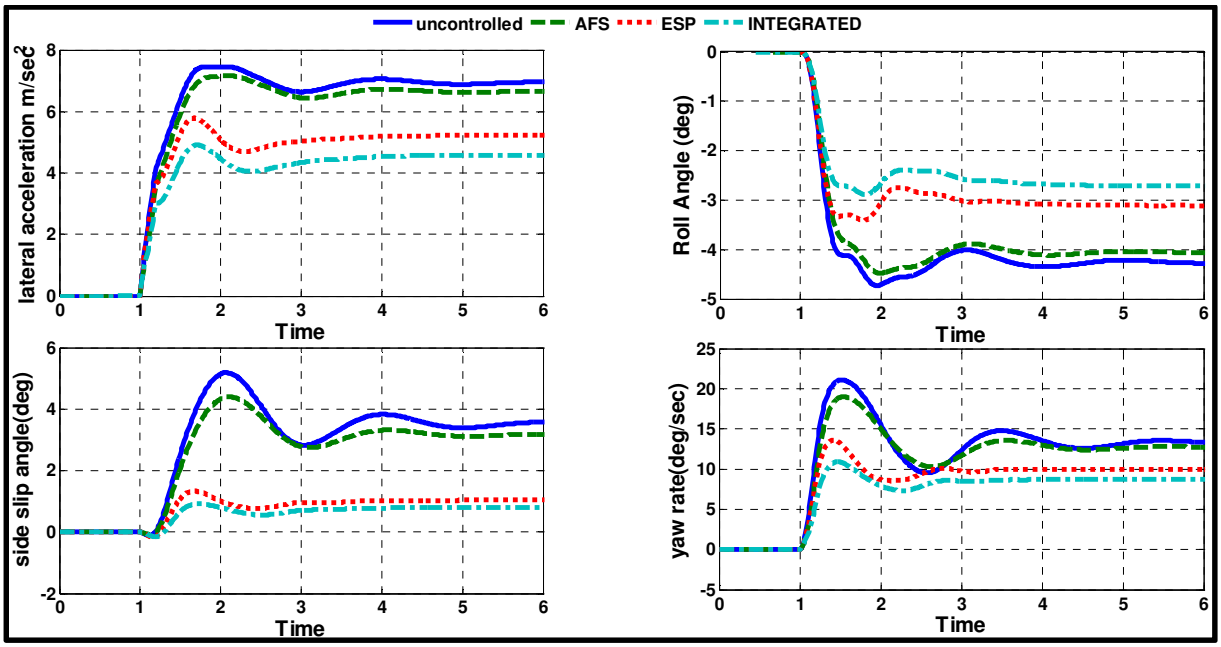

Fig. 9. Vehicle Response during J- turn with Speed 30 m/s.

Table 4. RMS for J Turn Steer Test at 30 m/s.

Criteria	Uncontrolled	AFS	ESP	Integrated
Lateral Acceleration	6.4991	6.2211 (**4.3%**)	4.8577 (**25.3%**)	4.229 (**35%**)
Side slip Angle	3.3586	3.0001 (**10.7%**)	0.9490 (**71.7%**)	0.7252 (**78.4%**)
Yaw Rate	12.9197	12.2914 (**4.9%**)	9.4312 (**27%**)	8.1921 (**36.6%**)
Roll Angle	3.9837	3.7923 (**4.8%**)	2.8866 (**27.6%**)	2.4935 (**37.5%**)

To demonstrate the effect of AFS control, ESP control, and integrated controller in preventing rollovers. The simulation is performed with steering input fishhook maneuver with maximum angle of 140 degree at speed 20 and 30 m/s respectively. The simulation results are depicted in Figs 10-11, which are reflecting a remarkable improvement in both vehicle handling and stability.

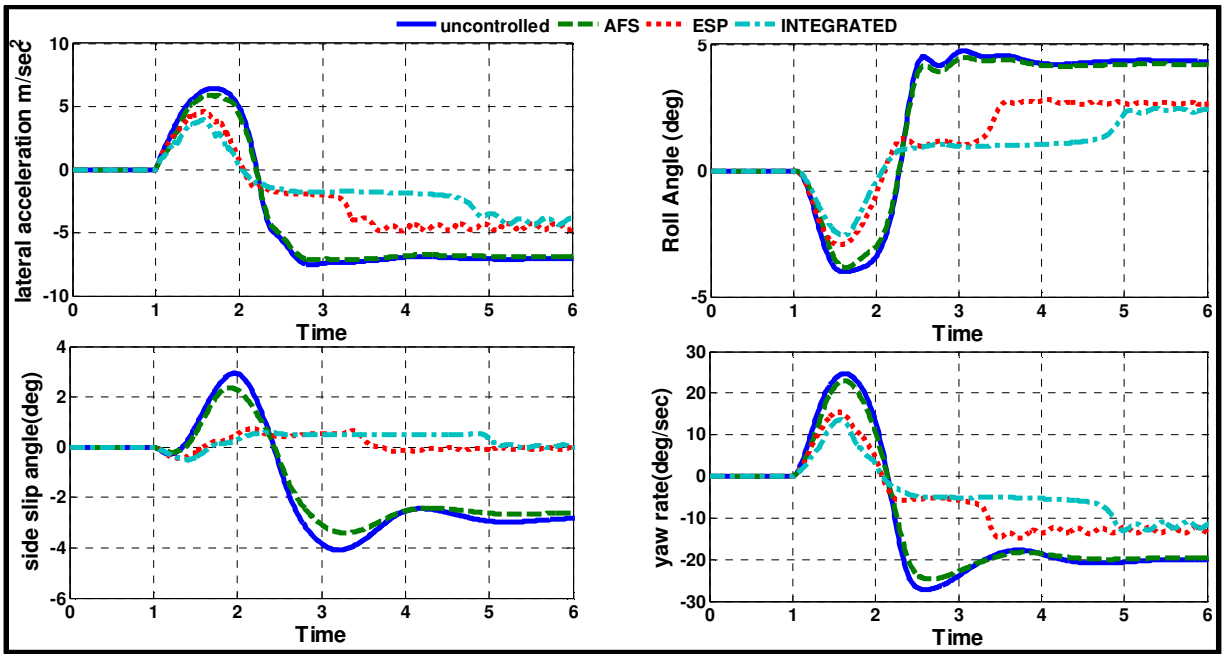

Fig. 10. Vehicle Response during Fishhook- turn with Speed 20 m/s.

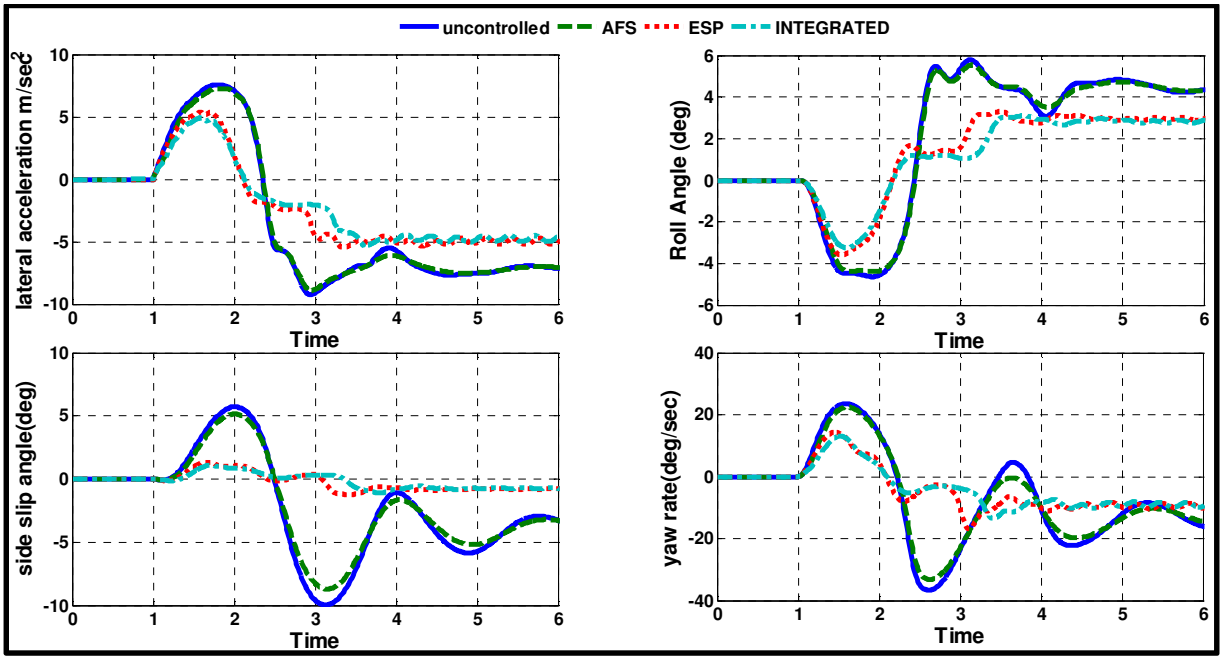

Fig. 11. Vehicle Response during Fishhook- turn with Speed 30 m/s.

It is clear from Figs 10-11 that, the AFS controller has almost no effect in high lateral acceleration with respect to the ESP controller, and integrated controller and the gain of the ESP controller need to be adjustable to avoid the nonhomogeneous. The root mean square values of the uncontrolled system, AFS only, ESP only, and integrated controller for fishhook turn maneuver at 30 m/sec are tabulated in Table 5.

Table 5. RMS for Fishhook Steer Test at 30 m/sec.

Criteria	Uncontrolled	AFS	ESP	Integrated
Lateral Acceleration	6.6708	6.5841(**1.3%**)	4.4158 (**33.8%**)	4.1257 (**38.2%**)
Side Slip Angle	4.3590	4.0355 (**7.4%**)	0.7514 (**82.8%**)	0.6539 (**85%**)
Yaw Rate	15.5319	14.7447 (**5.1%**)	8.8433 (**43.1%**)	8.1970 (**42.3%**)
Roll Angle	4.1553	4.0885 (**1.6%**)	2.6387 (**36.5%**)	2.4518 (**41%**)

Four stability indices for double lane-change maneuver ISO 3888-2 (2002) is shown in Figs 12-13 at speed 20 and 30 m/s respectively for the all systems. It is clear that there are a little difference in performance between AFS and ESP, but still integrated control is the best to cope the vehicle oscillations. The root mean square values of the uncontrolled, AFS only, ESP only, and integrated controller for double lane change maneuver at 30 m/sec are tabulated in Table 6.

Table 6. RMS for Double Lane Change Steer test at 30 m/s.

Criteria	uncontrolled	AFS	ESP	integrated
Lateral acceleration	2.8286	2.3024 (**18.6%**)	2.1860 (**22.7%**)	1.5536 (**45.1%**)
Side slip angle	1.0193	0.7630 (**25.2%**)	0.6201(**39.2%**)	0.3983 (**60.9%**)
Yaw rate	6.0880	4.8804 (**19.9%**)	4.6495 (**23.6%**)	3.2828 (**46.1%**)
Roll angle	1.7128	1.3866 (**19.1%**)	1.3119 (**23.4%**)	0.9291 (**45.8**)

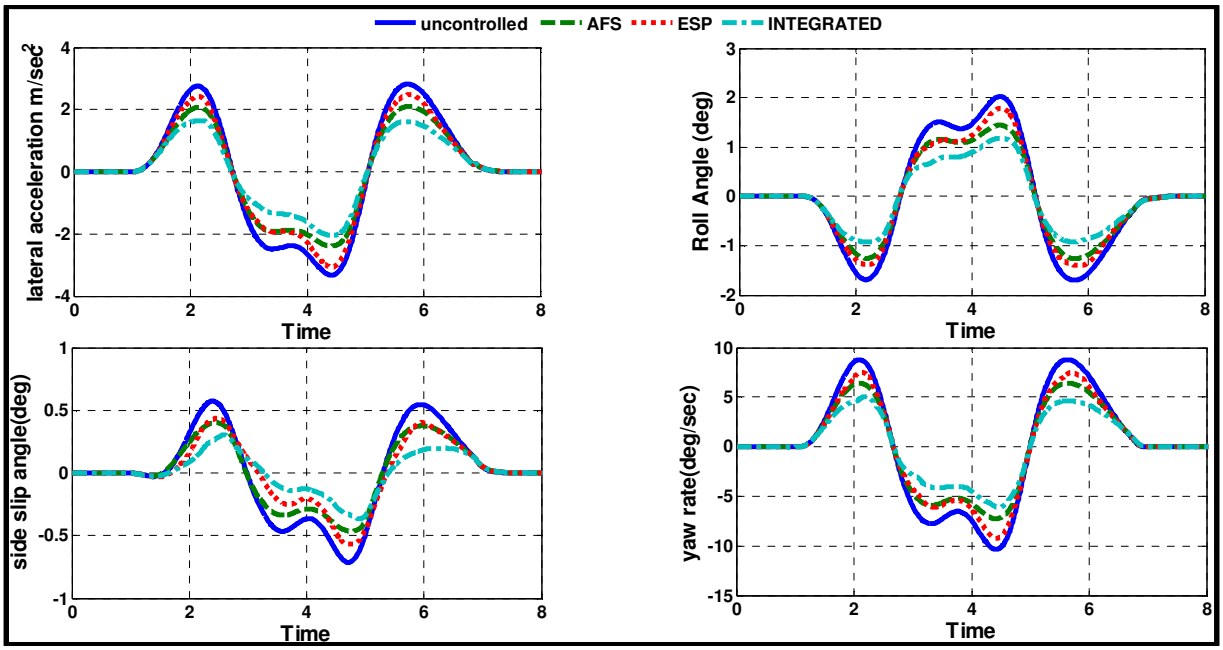

Fig. 12. Vehicle Response during double lane change with speed 20 m/s.

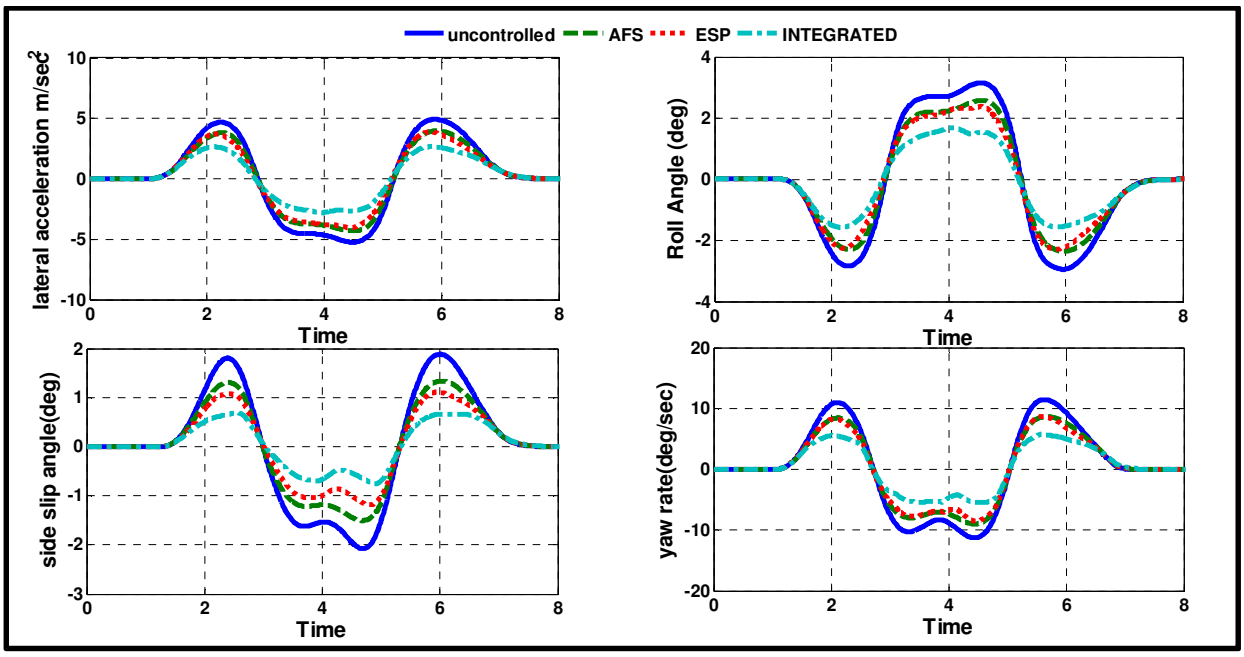

Fig. 13. Vehicle Response during double lane change with speed 30 m/s.

The above simulation results show that a vehicle equipped with the integrated control system can sustain its handling and stability in various hazardous conditions (different maneuvers) compared to the uncontrolled vehicle. In addition, the ESP control system can improve the vehicle response in high lateral acceleration while the AFS control system is more effective in law lateral acceleration of vehicle.

Finally, according to the simulation results, the integrated control give the best result compared to the other controllers, while the ESP control appear the significate results. In comparison to the well published literature for example in [17], the obtained results of the proposed controller are matched both in the qualitative and quantitative manner.

CONCLUSIONS

The presented paper proposed an integrated control system that integrates the active front steering (AFS) and active yaw moment control (ESP) with two fuzzy logic based controller to improve the vehicle handling, stability, and rollover prevention. The proposed control system generates corrective steering angle and differential braking for this purpose using yaw rate error, side slip angle error, and driver steering wheel angle as inputs.

The performance of the proposed system has been evaluated through numerical simulation of the mathematical model of a vehicle using MATLAB/Simulink. The fuzzy logic method based controller is shown to be an effective means of controlling vehicle handling and stability. The simulation results show that the AFS is more effective in law lateral acceleration, while the ESP is effective in all values of lateral acceleration, and the vehicle with the proposed integrated control system has smaller yaw rate, side slip angle, roll angle, and lateral acceleration than an uncontrolled vehicle for lane change, J turn, fishhook, and double lane change steer inputs with two different vehicle speeds.

REFERENCES

[1] Tahami, F., S. Farhangi, and R. Kazemi, '*A fuzzy logic direct yaw-moment control system for all-wheel-drive electric vehicles',* Vehicle System Dynamics, 2004. 41(3): p. 203-221.

[2] Li, L., et al., '*A novel fuzzy logic correctional algorithm for traction control systems on uneven low-friction road conditions',* Vehicle System Dynamics, 2015. 53(6): p. 711-733.

[3] Van Zanten, A.T., R. Erhardt, and G. Pfaff, *VDC, 'The vehicle dynamics control system of Bosch',* 1995, SAE Technical Paper.

[4] Kim, D., et al., '*Development of Mando ESP (electronic stability program)',* 2003, SAE Technical Paper.

[5] Anderson, J., '*Fuzzy Logic Approach to Stability Control*', 2010, PHD thesis, Clemson University.

[6] Yin, D. and J.-S. Hu, '*Active approach to Electronic Stability Control for front-wheel drive in-wheel motor electric vehicles',* International Journal of Automotive Technology, 2014. 15(6): p. 979-987.

[7] Petersen, I., '*Wheel slip control in ABS brakes using gain scheduled optimal control with constraints*', in *Department of Engineering Cybernetics. Norwegian University of Science and Technology, Trondheim, Norway*. 2003.

[8] Cheli, F., et al., '*A simplified ABS numerical model: Comparison with HIL and full scale experimental tests',* Computers & Structures, 2008. 86(13): p. 1494-1502.

[9] Aly, A., '*Intelligent fuzzy control for antilock brake system with road-surfaces identifier',* in *Mechatronics and Automation (ICMA), 2010 International Conference on*. 2010. IEEE.

[10] Sun, C. and X. Pei, '*Development of ABS ECU with Hardware-in-the-Loop Simulation Based on Labcar System',* SAE International Journal of Passenger Cars-Electronic and Electrical Systems, 2014. 8(2014-01-2524): p. 14-21.

[11] Wei, Z. and G. Xuexun, '*An ABS Control Strategy for Commercial Vehicle.* Mechatronics', IEEE/ASME Transactions on, 2015. 20(1): p. 384-392.

[12] Yao, Y., '*Vehicle steer-by-wire system control',* 2006, SAE Technical Paper.

[13] Mammar, S. and D. Koenig, '*Vehicle handling improvement by active steering',* Vehicle system dynamics, 2002. 38(3): p. 211-242.

[14] Wang, H., et al., '*Sliding mode control for steer-by-wire systems with AC motors in road vehicles',* Industrial Electronics, IEEE Transactions on, 2014. 61(3): p. 1596-1611.

[15] Abe, M., '*Vehicle dynamics and control for improving handling and active safety: from four-wheel steering to direct yaw moment control',* Proceedings of the Institution of Mechanical Engineers, Part K: Journal of Multi-body Dynamics, 1999. 213(2): p. 87-101.

[16] He, J., '*Integrated vehicle dynamics control using active steering, driveline and braking',* 2005, University of Leeds.

[17] Boada, M., et al., '*Integrated control of front-wheel steering and front braking forces on the basis of fuzzy logic',* Proceedings of the Institution of Mechanical Engineers, Part D: Journal of Automobile Engineering, 2006. 220(3): p. 253-267.

[18] March,C. and T. Shim, '*Integrated control of suspension and front steering to enhance vehicle handling',* ProceedingsoftheInstitutionofMechanical Engineers, Part D: Journal of Automobile Engineering, 2007. 221(4): p. 377-391.

[19] Li, D., S. Du, and F. Yu, '*Integrated vehicle chassis control based on direct yaw moment, active steering and active stabiliser',* Vehicle System Dynamics, 2008. 46(S1): p. 341-351.

[20] Rengaraj, C. and D. Crolla, '*Integrated chassis control to improve vehicle handling dynamics performance',* 2011, SAE Technical Paper.

[21] Feng, C., et al., '*Integrated control of automobile ABS/DYC/AFS for improving braking performance and stability',* International Journal of Vehicle Design, 2015. 67(3): p. 259-293.

[22] Karbalaei, R., et al., '*A new intelligent strategy to integrated control of AFS/DYC based on fuzzy logic',* International Journal of Mathematical, Physical and Engineering Sciences, 2007. 1(1): p. 47-52.

[23] Yihu, W., et al. '*A fuzzy control method to improve vehicle yaw stability based on integrated yaw moment control and active front steering',* in *Mechatronics and Automation, 2007. ICMA 2007. International Conference on*. 2007. IEEE.

[24] Li, B. and F. Yu, '*Design of a vehicle lateral stability control system via a fuzzy logic control approach',* Proceedings of the Institution of Mechanical Engineers, Part D: Journal of Automobile Engineering, 2010. 224(3): p. 313-326.

[25] Poussot-Vassal, C., '*Commande robuste LPV multivariable de chassis automobile*. 2008', Institut National Polytechnique de Grenoble-INPG.

[26] Baslamisli, S.Ç., İ.E. Köse, and G. Anlaş, '*Gain-scheduled integrated active steering and differential control for vehicle handling improvement',* Vehicle System Dynamics, 2009. 47(1): p. 99-119.

[27] Doumiati, M., Sename, O., Jairo, J., Molina, M., Dugard, L. and Poussot-Vassa, C., 'Gain-scheduled LPV/H∞ controller based *on direct yaw moment and active steering for vehicle handling improvements',* in *Decision and Control (CDC), 2010 49th IEEE Conference on*. 2010. IEEE.

[28] Doumiati, M., Sename, O., Dugard, L., Jairo, J., Molina, M., Gaspar, P., and Szabo, Z., '*Integrated vehicle dynamics control via coordination of active front steering and rear braking',* European Journal of Control, 2013. 19(2): p. 121-143.

[29] Yang, X., Z. Wang, and W. Peng, '*Coordinated control of AFS and DYC for vehicle handling and stability based on optimal guaranteed cost theory',* Vehicle System Dynamics, 2009. 47(1): p. 57-79.

[30] Sharaf, A., '*Real-time assessment of vehicle response in a virtual proving ground',* International Journal of Heavy Vehicle Systems, 2013. 20(2): p. 174-189.

[31] Ellis, J.R., '*Vehicle handling dynamics',* 1994.

[32] Pacejka, H., '*Tire and vehicle dynamics',* 2005: Elsevier.

[33] Rajamani, R., '*Vehicle dynamics and control',* 2011: Springer Science & Business Media.

APPENDIX-A

Table (A-1). Parameters of system model

Model parameters	Symbol	Value	Units
Total mass of the vehicle	M_t	1840.9	Kg
Sprung mass of the vehicle	M_s	1665.50	Kg
Front unsprung mass at each wheel	M_{wf}	44.83	Kg
Rear unsprung mass at each wheel	M_{wr}	41.42	Kg
Mass moment of inertia of the sprung mass about x axis	I_{xx}	734	Kg.m^2
Mass moment of inertia of the sprung mass about y axis	I_{yy}	3983	Kg.m^2
Mass moment of inertia of the sprung mass about z axis	I_{zz}	4240	Kg.m^2
Mass product moment of inertia of the vehicle sprung mass	I_{xz}	-15.6	Kg.m^2
Mass moment of inertia of wheels	I_{wi}	1.5	Kg.m^2
Stiffness coefficient of front suspension spring	K_f	20090	N/m
Stiffness coefficient of rear suspension spring	K_r	22700	N/m
Damping coefficient of front suspension	C_f	2000	N.s/m
Damping coefficient of rear suspension	C_r	2230	N.s/m
Cornering stiffness of front, rear tyres	$C_{\alpha f}$,αr	60000	N/rad
Distance from CG to the front axle	A	1.4499	m
Distance from CG to the rear axle	B	1.5801	m
Wheelbase (distance between front and rear axle)	L	3.030	m
Wheel track at front and rear axle	t_{rf} ,t_{rr}	1.558	m
Dynamic rolling radius of each wheel	r_{di}	0.3169	m